

Vibrational and Quantum-Chemical Study of Push – Pull Chromophores for Second-Order Nonlinear Optics from Rigidified Thiophene-Based π -Conjugating Spacers

Mari Carmen Ruiz Delgado,^[a] Víctor Hernández,^[a] Juan Casado,^[a]
Juan T. López Navarrete,^{*[a]} Jean-Manuel Raimundo,^[b] Philippe Blanchard,^[b] and
Jean Roncali^[b]

Abstract: Two types of push–pull chromophores built around thiophene-based π -conjugating spacers rigidified by either covalent bonds or noncovalent intramolecular interactions have been analysed by means of IR and Raman spectroscopical measurements in the solid state as well as in a variety of solvents. Comparison of the Raman features of NLO-phores based on a covalently rigidified dithienylene (DTE) spacer with those of their open chain DTE analogues shows that the bridging of the central double bond of DTE with the nearest β -positions of the thienyl units through two ethylene bridges significantly improves the intramolecular charge transfer. This also occurs for NLO-phores based on a 2,2'-bi(3,4-ethylenedioxythiophene) (BEDOT) spacer as compared with their corresponding parent compounds based on an unsubstituted bithiophene (BT)

spacer. For NLO-phores based on a BEDOT spacer, noncovalent intramolecular interactions between sulfur and oxygen atoms are responsible for the rigidification of the spacer. The Raman spectra of these NLO-phores obtained in the form of solutes in dilute solutions reveal two different behaviours: i) chromophores based on covalently bridged or open chain DTE spacers display Raman spectral profiles in solution quite similar to those of the corresponding solids, with a very little dependence on the polarity of the solvent, while ii) - larger spectral changes are noticed for NLO-phores built around BEDOT or BT spacers on going from solids to

solutions. In the second case, spectral changes must be ascribed not solely to conformational distortions of the donor and acceptor end groups with respect to the π -conjugated backbone mean-square-plane (as for the DTE-based NLO-phores) but also to distortions of the thienyl units of the π -conjugating spacer from coplanarity. The insertion of vinylenic bridges between the thienyl units of the π -conjugating spacer and between the spacer and the donor and acceptor end groups is a suitable strategy to reach a fairly large intramolecular charge transfer both in polar and non-polar solvents. Density functional theory (DFT) calculations have been carried out to assign the relevant electronic and vibrational features and to derive useful information about the molecular structure of these NLO-phores.


Keywords: density functional calculations • IR spectroscopy • nonlinear optics • push–pull oligomers • Raman spectroscopy

Introduction

Organic polymeric electrooptic materials are currently being investigated for their use in photonic devices in telecommunications and optical information processing.^[1] Usually, electrooptic materials involve a host polymeric matrix containing second-order nonlinear optical (NLO) chromophores either as guest molecules or covalently attached to the polymer backbone. The realization of a non-centrosymmetric active material requires the alignment of the dipole moments of the NLO-phores. Dipole orientation may be achieved by heating the polymer matrix containing the chromophore around the glass transition temperature (T_g) while maintaining an applied electric field during the cooling process. A major problem of such materials however involves the

[a] Prof. J. T. López Navarrete, Eng. M. C. Ruiz Delgado, Prof. V. Hernandez, Dr. J. Casado
Departamento de Química Física
Facultad de Ciencias, Universidad de Málaga
29071 Málaga (Spain)
Fax: (+34) 952-132000
E-mail: teodomiro@uma.es

[b] Dr. J.-M. Raimundo, Dr. P. Blanchard, Prof. J. Roncali
Groupe Systèmes Conjugués Linéaires
CNRS UMR 6501, Université d'Angers, 2 Bd Lavoisier
49045 Angers Cedex (France)

 Supporting information (Figure S1: B3LYP/3-21G eigenvectors calculated for the most intense skeletal C=C stretching vibrations of the four NLO-phores to illustrate the normal modes involved in the main Raman features.) for this article is available on the WWW under <http://www.chemeurj.org/> or from the author.

structural relaxation of the chromophores with progressive return to an head-to-tail orientation of the dipoles resulting in a loss of NLO activity. While the use of high T_g polymer matrixes represents a possible solution, this in turn imposes stringent prerequisites regarding the chemical and thermal stability of the incorporated NLO-phores.^[1]

Dipolar push–pull chromophores likely constitute the widest class of compounds investigated for their NLO properties.^[2–11] These push–pull NLO-phores are basically constituted by an electron-donor and an electron-acceptor as groups which interact through a π -conjugating spacer. It is already well-known that the hyperpolarizability (β), which characterizes the molecular NLO efficiency, depends on the strength of the donor and acceptor groups, on the extent of the π -conjugated path and, for conjugating spacers based on aromatic units, on the resonance stabilization energy of the aromatic system.^[4]

Polyenic systems represent in principle the most effective way to achieve charge redistribution between the donor and the acceptor end groups. Consequently, push–pull polyenes have been shown to exhibit huge nonlinearities;^[5] however, the well-known limited chemical and photothermal stability of extended polyenes might represent an obstacle to the practical applications of the derived NLO-phores. However, the large aromaticity of the benzene ring has a detrimental effect on the second-order polarizabilities.

Since the aromaticity of thiophene is lower than that of benzene and the stability and solubility of thiophene derivatives higher than that of the polyene compounds, much attention has recently been paid to NLO-phores that contain thiophene.^[5a, 12] Some of us have recently reported on a novel synthetic approach for the design of stable thiophene-based second-order NLO-phores with improved nonlinearities. To this end, two series of push–pull chromophores derived from rigidified π -conjugated spacers were synthesized.^[13–15] The rigidification of the π -conjugated backbone was performed either by covalently bridging appropriate positions of the thiophene-based spacer or by taking advantage of intramolecular noncovalent interactions occurring in π -conjugated oligomers and polymers containing 3,4-ethylenedioxythiophene (EDOT) units.

Rigidified push–pull chromophores of the first series were built around a 6,6'-bis(4,5-dihydro-6*H*-cyclopenta[*b*]-thienylidene) π -conjugated spine (i.e., a covalently bridged dithienylene, DTE, spacer)^[13] while the members of the second series of push–pull NLO-phores were derived from a 2,2'-bi(3,4-ethylenedioxythiophene) (BEDOT) π -conjugating spacer.^[14] Despite the markedly different chemical structures, the two series of systems have in common the fact that they represent rigidified versions of the parent structures namely, open chain DTE in the first case and bithiophene (BT) in the second one.

Vis-NIR electronic absorption and IR and Raman spectroscopical measurements have been successfully used as complementary techniques to study many different classes of π -conjugated polymers and oligomers, which show strong electron-phonon coupling due to their quasi one-dimensional structures. Raman spectroscopy has been shown to be a particularly powerful tool in: i) estimating the efficiency of

the π -conjugation in the neutral state,^[16–18] ii) characterizing different types of conjugational defects in doped π -conjugated materials,^[19] and iii) analyzing the intramolecular charge transfer in push–pull π -conjugated oligomers.^[20, 21] On the basis of the effective conjugation coordinate (ECC) theory,^[22] the appearance of only a few, overwhelmingly strong, Raman bands is consequence of the existence of an effective electron-phonon coupling over the whole π -conjugated backbone of the molecule. In aromatic and heteroaromatic polyconjugated systems, the collective ECC vibrational coordinate has the analytic form of a linear combination of ring C=C/C–C stretchings which points in the direction from the benzenoid structure (usually that of the ground state) to the quinonoid structure (that corresponding to the electronically excited state or the oxidized species). The ECC formalism states that when the conjugation length (CL) increases, the totally-symmetric normal modes of the neutral system involved in the molecular dynamics of the ECC coordinate (i.e., those giving rise to the few Raman bands experimentally observed) undergo sizeable dispersions both in frequency and intensity. Changes in the peak positions of the Raman bands upon chain elongation are particularly useful in evaluating the CL in a homogeneous series of neutral oligomers. On the other hand, when conjugated oligomers and, in particular, oligothiophenes become oxidized (either chemically or electrochemically) or photoexcited, typically, quinonoid structures are created.^[23] These structural modifications also produce a significant downshift of the Raman bands associated to the π -conjugated path. The evolution of the Raman spectral profile between the neutral and the different doped states is a useful tool for elucidating the type of charged carriers created upon oxidation.^[16–19]

In this work, we focus on the electronic and vibrational (IR and Raman spectra), both in solid state and in a variety of solvents, of some representative members of the above series of push–pull chromophores containing rigidified DTE or BEDOT thiophene-based spacers. Comparisons of the Raman features will be made between solids and solutes, and between the rigidified DTE and BEDOT NLO-phores with their open chain DTE and unsubstituted bithiophene analogues to analyze, at the molecular level, the effects of the rigidification of the spacer on the intramolecular charge transfer (ICT) from the electron donor to the electron acceptor groups. The IR-active $\nu(\text{CN})$ stretchings of the selected NLO-phores, all of them containing a dicyanomethylene moiety as the electron acceptor end group, are also expected to be sensitive to the degree of intramolecular charge transfer. Density Functional Theory (DFT) calculations have been carried out as a guide for the analysis of the electronic and vibrational spectra and to derive relevant molecular parameters regarding bond lengths and the atomic charges distribution.

Results and Discussion

Synthesis and UV/Vis absorption maxima: The chemical structures and abbreviate notation of the NLO-phores studied in this article are depicted in Figure 1. The chromophores bear

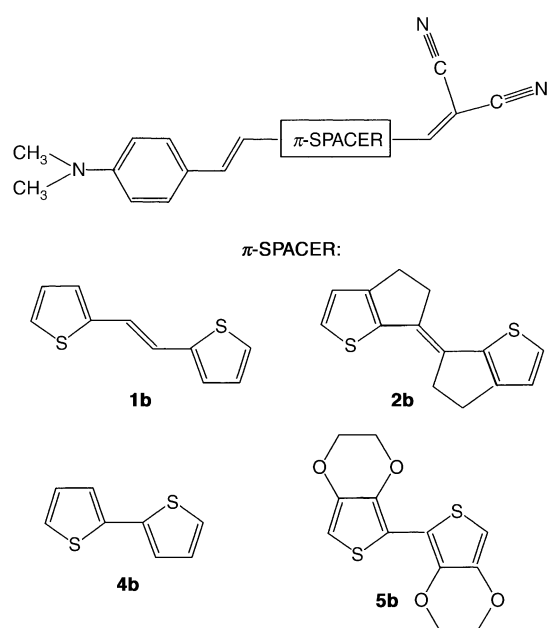


Figure 1. Chemical structures and abbreviate notation to be used throughout the text.

an *N,N*-dimethylaniline group as the electron donor and an acceptor group derived from malonitrile. All these NLO-phores were prepared according to a general synthetic methodology involving i) monoformylation of the π -conjugating spacer by Vilsmeier reaction, ii) introduction of the donor group by Wittig olefination of the resulting aldehyde, iii) second monoformylation, and iv) Knoevenagel condensation between the resulting aldehyde compound and the malonitrile acceptor with an active methylene group. Whereas NLO-phores **2b** and **5b** have been previously prepared,^[13–15] the synthesis of **1b** and **4b** is reported here for the first time.

Except for the commercially available BT (**4**), the various π -conjugating spacers were synthesized following known procedures. DTE (**1**) of *E* configuration was prepared by McMurry coupling of 2-thiophenecarboxaldehyde,^[24] whereas the covalently bridged analogue **2** was obtained in four steps from 3-(3-thienyl)acrylic acid according to the already reported procedure.^[25] BEDOT (**5**) was prepared by oxidative coupling of the lithio derivative of the commercially available EDOT in the presence of CuCl_2 .^[26]

The *N,N*-dimethylaniline electron donor was introduced via a phosphonium iodine obtained in an one-step reaction involving treatment of freshly distilled *N,N*-dimethylaniline by triphenylphosphine, potassium iodine, and formaldehyde.^[27] All π -conjugating spacers were subjected to a Vilsmeier reaction in the presence of POCl_3 and DMF in refluxing anhydrous 1,2-dichloroethane, affording selectively aldehydes in good yield (80–94%). Subsequent Wittig olefination with the *N,N*-dimethylaniline phosphonium salt in the presence of potassium *tert*-butylate led to the corresponding electron donor-substituted compounds (68–97% yields) as a mixture of *E* and *Z* isomers. The pure *E* isomer could be isolated by column chromatography on silica gel followed, when necessary, by a further purification by precipitation of the less soluble *E* isomer. However, it was still possible to directly use

the *E/Z* mixture in the subsequent Vilsmeier formylation since isomerization to the *E* isomer occurred in the conditions of the reaction.

Formylation of the unsubstituted end α -position of the various electron donor-substituted π -conjugating spacers was achieved by treatment of the compounds by 1 equiv *n*BuLi, followed by addition of DMF and hydrolysis (in the case of **1b**) and using a Vilsmeier reaction (in the case of **4b**). The $^1\text{H NMR}$ analysis of the four aldehyde compounds shows that the $\text{C}=\text{C}$ double bonds connecting the electron donor to the π spacer are in *E* configuration as confirmed by a coupling constant $J \approx 16$ Hz between the two corresponding protons.

The final Knoevenagel condensation for the incorporation of the electron acceptor moiety derived from malonitrile to the aldehyde compounds was performed by refluxing chloroform in the presence of triethylamine. NLO-phores **1b** and **4b** were obtained as dark or dark-blue powders.

Table 1 lists the UV/Vis absorption maxima (λ_{max}) of the NLO-phores **1b**–**5b** in a variety of solvents with different polarities. Comparison of the data for **1b** and **2b** shows that

Table 1. UV/Vis absorption maxima (λ_{max}) of the NLO-phores **1b**–**5b** in various solvents.

Compound	Dioxane ^[a]	CH_2Cl_2 ^[a]	DMSO ^[a]
1b	544	560	560
2b	584	614	615
4b	528	548	550
5b	573	588	594

[a] λ_{max} values in nm.

the bridging of the central double bond of DTE with the nearest β -positions of the thienyl units through two ethylene bridges significantly improves the ICT, as evidenced by the considerable bathochromic shift of λ_{max} in solution (i.e., 40 nm in dioxane and 54 nm in CH_2Cl_2 and DMSO). This effect however is not solely due to the rigidification of the π -conjugating system, but mainly to the strong inductive donor effect of methylene groups of the bridges (see below the analysis of the Raman spectra of the corresponding DTE spacers).

Single crystal X-ray crystallographic data for the BEDOT spacer revealed the occurrence of strong $\text{S}\cdots\text{O}$ intramolecular interactions.^[14] The persistence of a nearly *anti*-coplanar conformation of the EDOT subunits of the BEDOT spacer in solution is supported by several electronic absorption data.^[15, 28] Although BT is known to be a less efficient electron relay than DTE, due to the combined effects of a less planar and more aromatic structure (as showed by the absorption maxima of **1b** and **4b**), NLO-phores based on BT present the advantage of an easier synthetic access. Comparison of the λ_{max} values for **5b** with **1b** and **2b** shows that BEDOT leads to an efficient ICT comparable to that of the open chain DTE but lower than the covalently bridged DTE. Of course, however, due to the electron-releasing effect of the ethylenedioxy groups, the BEDOT spacer cannot be simply considered as a rigidified version of the BT π -conjugating spacer.

Optimized geometries and electronic spectra: Figure 2 shows, from a simple chemical point of view, the two limiting resonant forms which enter with different weights into the stabilization of the electronic structure of a push–pull π -conjugated oligomer. The neutral form **A** implies that no intramolecular charge transfer takes place from the donor to the acceptor, and the spacer displays a full aromatic structure. On the other hand, in the charge-separated state **B** one electron is fully transferred from the donor to the acceptor, and the π -conjugating spacer becomes fully quinoidized.

The main factors which determine the degree of polarization of the π -electrons cloud of the spacer are: i) the strength of the donor and acceptor end groups, and ii) the chemical nature of the spacer (i.e., oligoenes, oligothiophenes, oligothiophenylvinyls, etc.) iii) and the number of units in the π -conjugated chain. The first consequence of the existence in the push–pull oligomer of an efficient ICT is the appearance of a molecular dipole moment (generally large) directed from the acceptor to the donor, where the value becomes larger as the polarization of the molecule increases. A second consequence involves the molecular geometry of the spacer. The actual electronic structure of a push–pull π -conjugated oligomer can be considered, at first glance, to result from a linear combination of the two limiting resonant forms plotted in Figure 2. The relative stability of the zwitterionic form **B** with respect to the neutral form **A** determines the weights of both canonical structures into the linear combination which describes the structure of the molecule.

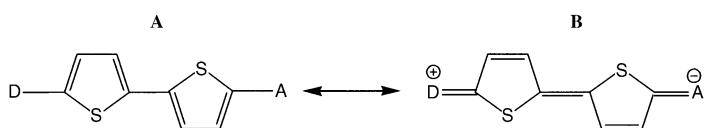


Figure 2. Neutral and charge-separated limiting resonant forms for the class of push–pull oligothiophenes.

To obtain a further understanding on the equilibrium molecular geometries and charge distributions, we have performed optimizations, within the framework of the density functional theory, for the four NLO-phores studied in this paper using the *ab initio* B3LYP/6-31G* model chemistry. Figure 3 displays the main skeletal bond lengths for compounds **1b** and **2b** (those for **4b** and **5b** are available upon request to the authors).

In view of the optimized DFT//B3LYP/6-31G* molecular geometries of these NLO-phores, one observes that the conjugated C=C/C–C bonds of the acceptor subunit are mainly affected by the electronic interaction with the electron withdrawing end group, whereas those of the donor subunit are less affected by the interaction with the electron-donating group. For compound **1b**, the mean single-double C–C bond length alternation pattern (BLA) of the thiophene rings attached to the donor and to the acceptor amount 0.022 and 0.006 Å, respectively; while the corresponding values for the other NLO-phores are: 0.021 and –0.004 Å (**2b**), 0.025 and 0.006 Å (**4b**), 0.020 and 0.001 Å (**5b**). These BLA values, related to the difference between the average length of single

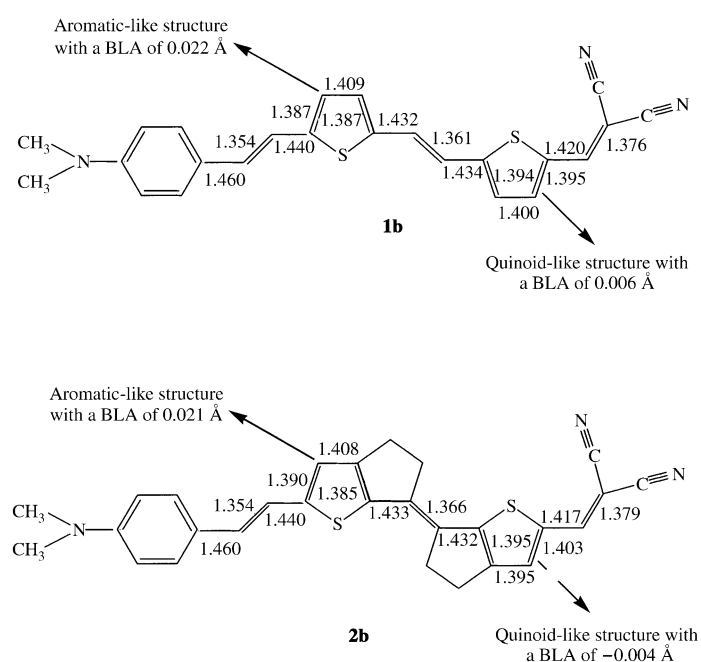


Figure 3. DFT//B3LYP/6-31G* optimized skeletal bond lengths for compounds **1b** and **2b**.

and double bonds, can be compared with the about 0.07 Å commonly found from experiments for the central rings of the neutral non-polar oligothiophenes.^[29–32] Thus, the attachment of the electron withdrawing malonitrile group to any of the four π -conjugating spacers studied here induces a sizeable quinoidization of the acceptor-substituted thiophene ring (particularly in the cases of the covalently bridged DTE and BEDOT spacers, namely for NLO-phores **2b** and **5b**); although the geometrical modifications due the strong polarization of the π -electrons cloud quickly decrease away from the acceptor group. We also observe that the C–S bonds undergo sizeable variations from one NLO-phore to another due to steric hindrance or electrostatic interactions with the substituents. As a result, which is in contrast with the simple chemical point of view of the balance between the two limiting resonant forms briefly summarized above, the existence in this class of push–pull π -conjugated oligomers of an efficient ICT translates into a larger perturbation of the acceptor subunit than that of the donor subunit, thus generating two different molecular domains within the π -conjugating spacer (one of them bearing a partial quinoid character while the other still retains a partial aromatic character). The structural modifications induced by the attachment of strong electron withdrawing groups are expected to extend towards the middle of the π -conjugating spacer as its chain length becomes longer, due to the increasing molecular polarizability.

Figure 4 shows the natural bond orbital atomic charges over the donor and acceptor groups for **1b** and **4b** NLO-phores and each of the molecular domains which can be hypothesized within the π -conjugating spacer. DFT//B3LYP/6-31G* model chemistry reveals an interesting difference with respect to the rather simple charge distribution associated to the zwitterionic canonical form (i.e., with respect to form **B** in Figure 2).

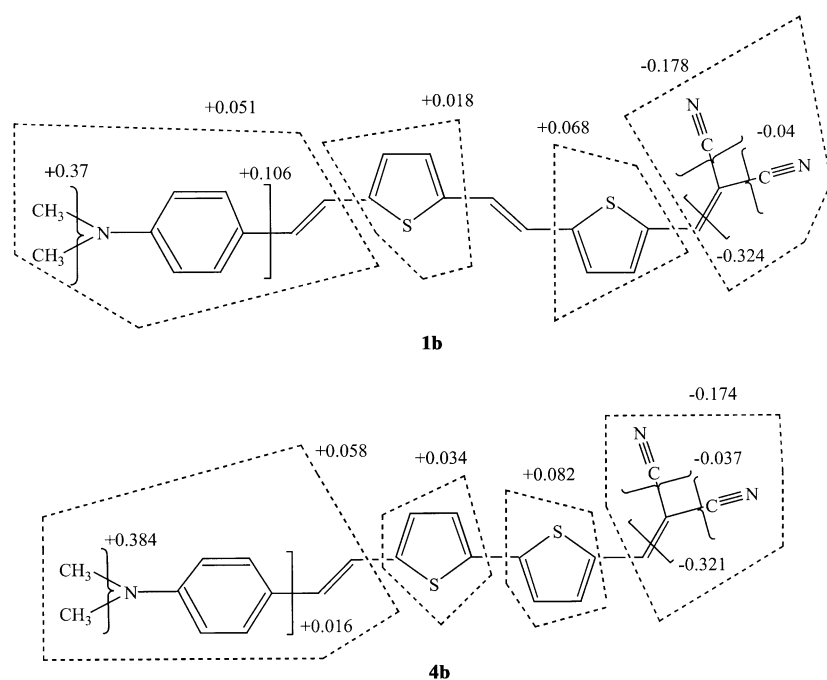


Figure 4. Natural bond orbital atomic charges for compounds **1b** and **4b** as deduced from their optimized DFT//B3LYP/6-31G* molecular geometries.

Thus, the natural population atomic charges over the donor and the acceptor end groups amount +0.051 and -0.178 e, respectively for **1b**, whereas for **4b** the corresponding values are +0.058 and -0.174 e. The charge distributions for **2b** and **5b** display a similar behaviour, although the specific values are not reported here for simplicity. Anyway, B3LYP/6-31G* calculations indicate that the charge over the malonitrile group is around 3–3.5 times higher than that on the *N,N*-dimethylaniline group, and that the π -conjugating spacer is highly polarized since it bears nearly the 65–70% of the net positive charge of the whole molecule (likely due to the strong interaction with the acceptor group). Thus, for **1b** the net charges over the thieryl rings of the open chain DTE spacer attached to the donor and to the acceptor end groups, respectively, amount +0.018 and +0.068 e (without taking into account the net positive charge over the central vinylenic bond), whereas for **4b** NLO-phore the corresponding values for each thieryl ring of the BT spacer are +0.034 and +0.082 e.

To rationalize the evolution of the electronic absorption properties in the push–pull materials, the electronic spectra of the four NLO-phores were calculated at the B3LYP/6-31G* level within the time-dependent DFT (TDDFT) approach. TDDFT calculations predict one intense electronic transition at 2.23 eV (with oscillator strengths $f=1.54$), 2.21 eV ($f=1.68$), 2.39 eV ($f=1.35$) and 2.34 eV ($f=1.48$) for **1b**, **2b**, **4b** and **5b**, respectively, in good accordance with the experimental data. In all the cases, this electronic absorption corresponds to the transition from the ground to the first excited state and is mainly described by one-electron excitation from the highest occupied molecular orbital (HOMO) to the lowest unoccupied molecular orbital (LUMO). The intense absorption observed around 550 nm in the four

NLO-phores is therefore assigned to the HOMO \rightarrow LUMO one electron promotion calculated at around 2.2 eV.

The atomic orbital composition of the frontier molecular orbitals is sketched in Figure 5. For the four molecules studied in this work, the HOMO is of π nature and is delocalized along the CC backbone (with a small contribution of the thiophene ring linked to the acceptor group) and on the *N,N*-dimethylaniline electron donor group. By contrast, the LUMO is concentrated on the malonitrile acceptor group and extends to the nearest thiophene ring. Consequently, the HOMO \rightarrow LUMO transition implies an electron density transfer from the more aromatic domain of the π -conjugating spacer including the electron donor group, to its more quinonoid side and mainly to the electron-withdrawing group. The topology of the frontier molecular orbitals thus demonstrate the charge-transfer character of the HOMO \rightarrow LUMO transition. Moreover, these orbitals topologies show the HOMO–LUMO overlap that is a prerequisite to increase the easiness of the charge transfer transition and, consequently, the nonlinear optical response.

The topology of the frontier molecular orbitals thus demonstrate the charge-transfer character of the HOMO \rightarrow LUMO transition. Moreover, these orbitals topologies show the HOMO–LUMO overlap that is a prerequisite to increase the easiness of the charge transfer transition and, consequently, the nonlinear optical response.

Experimental and theoretical IR and Raman spectra: Figure 6 shows the comparison between the IR and Raman spectra of **4b**, as the prototypical example for the push–pull materials, and of an α,α' -bisphenyl end-capped bithiophene, as the prototypical example for the non-polar π -conjugated materials. A few vibrational spectroscopic observations, of general validity, which differentiate the two classes of π -conjugated materials (i.e., push–pull and non-polar) are the following:

- As mentioned in the introductory section, the Raman spectra of the non-polar π -conjugated oligomers display a surprisingly simple appearance, and only three or four lines, associated to particular totally symmetric skeletal CC vibrations, are recorded with overwhelmingly intensity in the 1600 and 1000 cm^{-1} region, as a result of the strong electron-phonon coupling, which takes place in this type of systems due to their quasi one-dimensional structure.^[16–22]
- More than three or four strong bands are observed in the Raman spectra of the push–pull oligomers due to the lowering of the molecular symmetry. In general, the additional lines arise from the vibrational coupling of the π -conjugating spacer with stretching vibrations of the end groups.^[20–22]
- The large molecular dipole moment directed from the acceptor to the donor makes the same vibrational normal modes of the π -conjugated backbone giving rise to the

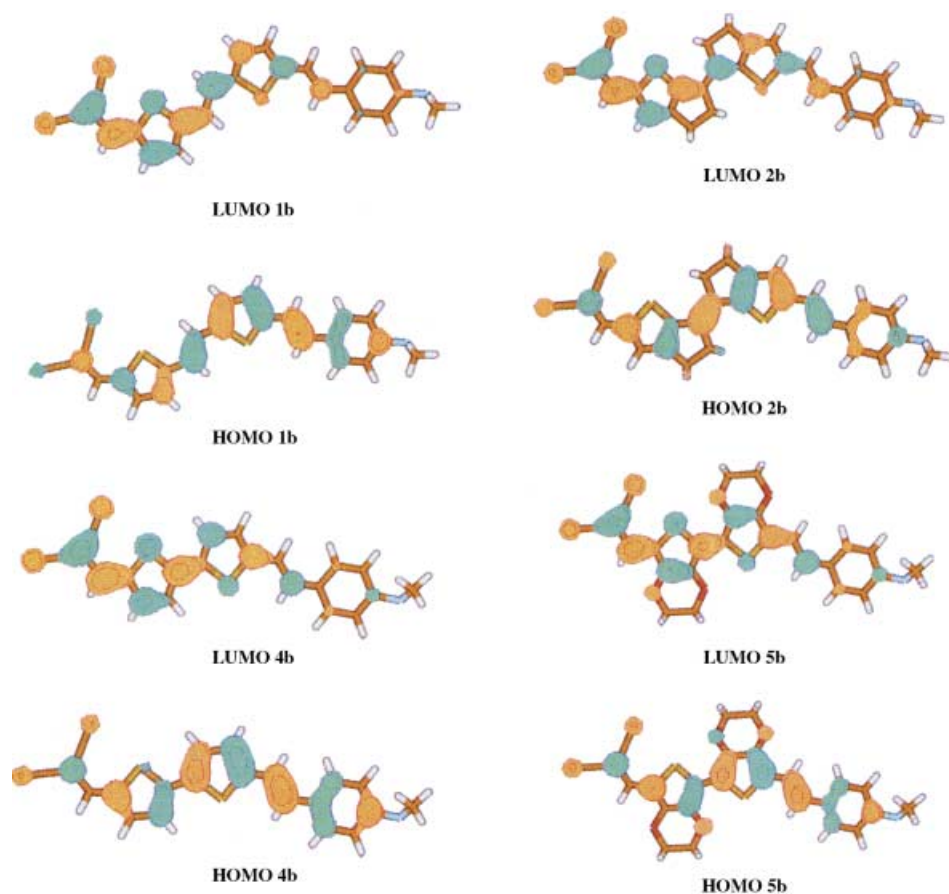


Figure 5. Electronic density contours (0.03 e bohr^{-3}) calculated for the HOMO and LUMO frontier molecular orbitals of **1b**, **2b**, **4b** and **5b**.

Raman bands experimentally observed to gain also an extra-large IR-activity due to the sizeable fluxes of charge induced along the strongly polarized alternating sequence of double/single C–C bonds. This is not the case for the centrosymmetric non-polar oligothiophenes, for which the mutual exclusion principle holds due to the existence of an inversion center in the middle of the system, so that the Raman-active vibrations become undetectable in the IR spectrum, and viceversa. In addition, for the non-polar oligothiophenes, the out-of-plane γ (C–H) bending vibrations, appearing around 800 cm^{-1} , are by far the strongest IR absorptions (see Figure 6). Thus, for a push–pull material, the resemblance between the IR and Raman spectra can be used as a proof that an effective ICT takes place.^[20–22]

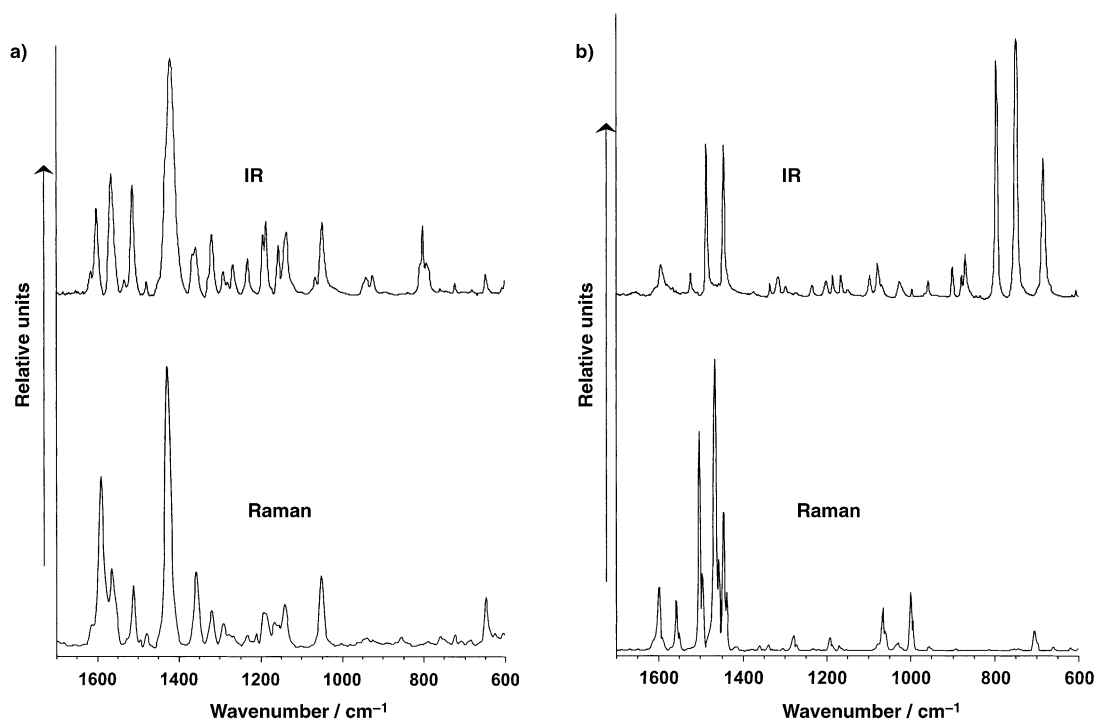


Figure 6. Comparison between the IR and Raman spectra of: a) **4b** as the prototypical example for a push–pull material and b) α,α' -bisphenyl end-capped bithiophene (P-2T-P) as the prototypical example for the nonpolar π -conjugated materials.

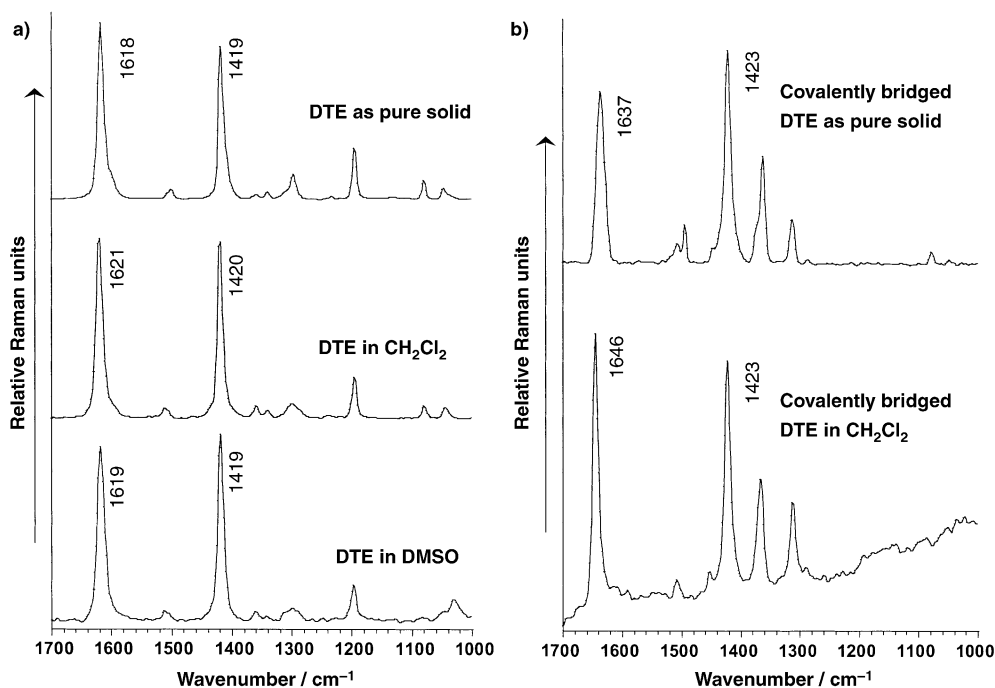


Figure 7. Raman spectra of a) open chain DTE spacer in solid state and in dilute CH_2Cl_2 and DMSO solutions and b) covalently bridged DTE in solid state and dilute CH_2Cl_2 solution.

Let us now proceed with the Raman spectral analysis of the unsubstituted π -conjugating spacers used here. Figure 7 shows the Raman spectra of the open chain and covalently bridged DTE spacers, in the solid state and as solutes in dilute solutions. The π -conjugating spacer **1** displays almost the same spectral profile (both in peak positions and relative intensities) as a solid sample than as a solute in CH_2Cl_2 and DMSO solutions. This experimental finding demonstrates that π -conjugation is the driving force which determines that the distortions from coplanarity of the thiophene rings of DTE are not too large, neither in solid state nor in solution.

On the other hand, the shifts of the Raman lines at 1637 and 1423 cm^{-1} of spacer **2** with respect to their counterparts in spacer **1** at 1618 and 1419 cm^{-1} (lines which are associated to the $\nu(\text{C}=\text{C})$ stretchings of the central vinylenic bond and of the two thiophene rings, respectively) reveals that the covalent rigidification of DTE renders a spacer richer in π -electrons than its open chain analogue. The reason for this must be found in the strong inductive donor effects of the methylene groups attached at the β -positions of the thiophene rings. Curiously, even if spacer **2** was conceived as a rigidified version of spacer **1**, the shift of the Raman band at 1637 cm^{-1} by near 10 cm^{-1} upon solvation in dichloromethane suggests that the interaction between the solvent and the methylene groups of the two intramolecular bridges leads to a slight conformational distortion of the π -conjugated spine from coplanarity so that the overlapping between the sp^2 orbitals of the successive constituting units decreases with respect to the solid state, contrarily to what found for the open chain DTE spacer, for which the solvents effects are negligible.

Figure 8 compares the Raman spectra of the various NLO-phores (obtained in the form of pure powders) with the corresponding B3LYP/3-21G* model spectra. The agreement

between theory and experiments is remarkably satisfactory for all compounds. Nonetheless, the complete assignment of the IR and Raman bands of each NLO-phore to particular vibrations is beyond the scope of our analysis. We will restrict our discussion only to the more relevant observations.

The Raman bands at 1593 (**1b**) and 1600 cm^{-1} (**2b**) are due to the pure $\nu(\text{C}=\text{C})$ stretching of the central vinylenic bond of the chromophore, and can be correlated with their counterparts in the corresponding unsubstituted π -conjugating spacers: 1618 cm^{-1} for open chain DTE and 1637 cm^{-1} for covalently bridged DTE (the corresponding eigenvectors for **1b** and **2b** are plotted in Figure S1, Supporting Information). The dispersion towards lower frequencies of this stretching normal vibration (i.e., by 25 cm^{-1} for **1b** and by 37 cm^{-1} for **2b**) is indicative of a sizeable softening of the π -conjugated backbone upon appending electron-active donor and acceptor groups at the end α,α' -positions of the spacer. The larger downshift for **2b** than for **1b** agrees both with the bathochromic shift of the UV/Vis absorption maxima (λ_{max}) in solution and with the lower BLA values (particularly for the acceptor-subunit) deduced from the B3LYP/6-31G* model chemistry of the former NLO-phore as compared with the latter one.

The strongest Raman band for each chromophore is that appearing at: 1411 (**1b**), 1400 (**2b**), 1428 (**4b**) and 1430 cm^{-1} (**5b**). The B3LYP/3-21G* eigenvectors reveal that these lines arise from the same $\nu(\text{CC})$ stretching vibration: a *collective oscillation of the whole alternating sequence of C=C/C-C bonds*, along which all conjugated C=C bonds lengthen in-phase while all conjugated C-C bonds shrink in-phase (see Figure S1 in Supporting Information). This characteristic *collective skeletal vibration* mimics the change of the nuclear configuration of the NLO-phore in going from a *heteroar-*

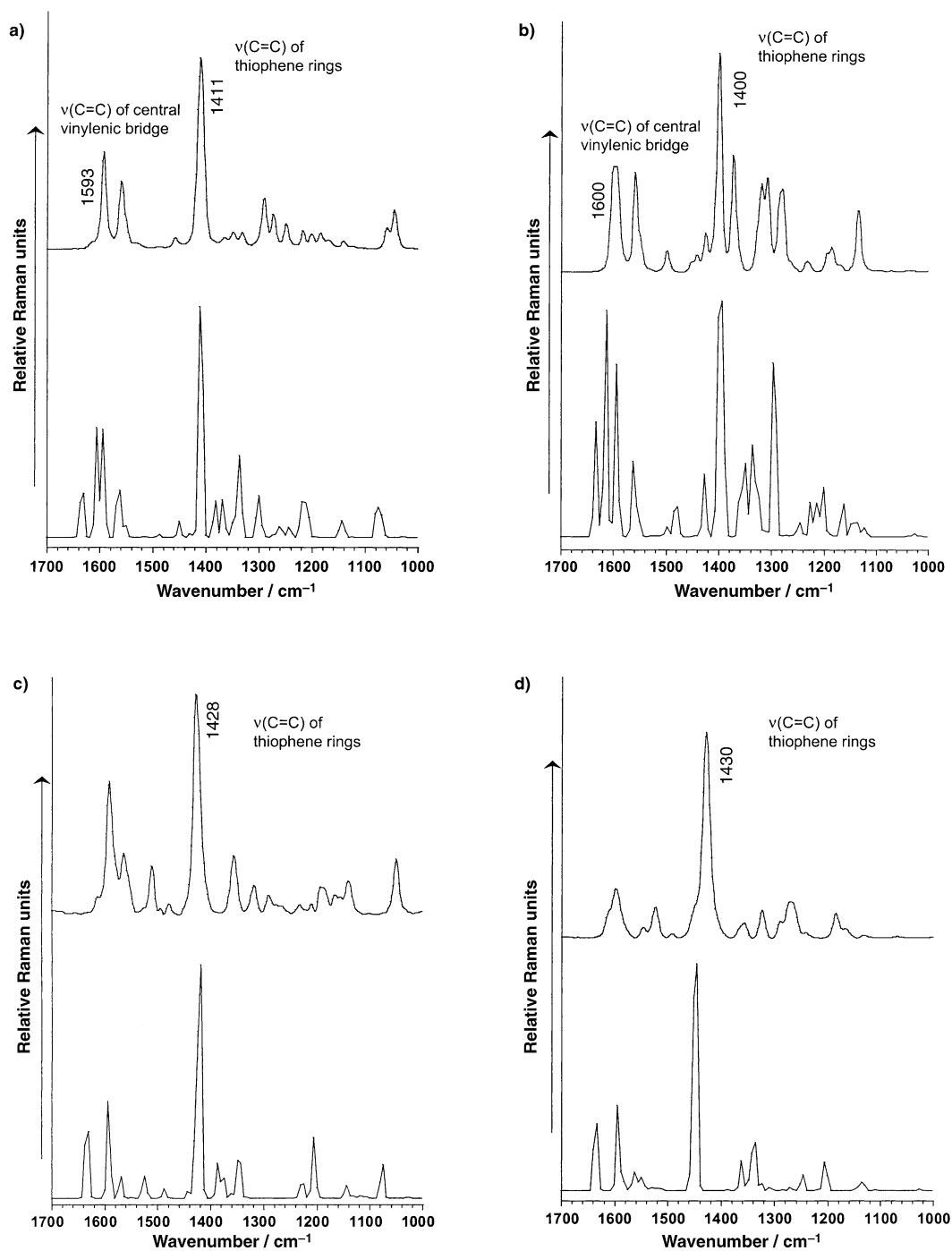


Figure 8. Comparison between the experimental (solid state) and B3LYP/3-21G* theoretical Raman spectra of NLO-phores: a) **1b**, b) **2b**, c) **4b** and d) **5b**.

omatic structure of the π -conjugated system to a *heteroquinonoid* one, and it is usually termed as the \mathfrak{R} “mode” in the ECC theory.^[22] As for the unsubstituted π -conjugating spacers, the B3LYP/3-21G* calculations indicate that the \mathfrak{R} mode corresponds to the Raman scatterings at: 1419 (open chain DTE), 1423 (covalently bridged DTE), 1442 (BT) and 1452 cm^{-1} (BEDOT). The redshift of the \mathfrak{R} mode upon attaching the electron donating *N,N*-dimethylaniline and the electron withdrawing malonitrile end groups to the spacer (i.e., 8 cm^{-1} for **1b**, 23 cm^{-1} for **2b**, 14 cm^{-1} for **4b** and 22 cm^{-1} for **5b**) is in full agreement with the predictions of the

ECC model^[22] and with what experimentally found for the neutral and doped forms of the oligothiophenes.^[18, 19] The strongest line in the Raman spectra of the neutral (non-polar) forms of a series of α,α' -dimethyl end-capped oligothiophenes^[18a] occurred at around 1480 cm^{-1} (which is characteristic of the *heteroaromatic* structure of the π -conjugated backbone), while it largely downshifted upon ionization of the π -conjugated backbone, splitting into two components at around 1440 and 1420 cm^{-1} (being typical markers of the attainment of a *heteroquinonoid* structure of the π -conjugated backbone). The relative intensities of these two bands are

indicative of the degree of quinoidization of the π -conjugated backbone: that at 1440 cm^{-1} is stronger for the radical cationic species (for which the quinoidization mainly affects the middle part of the molecule),^[19a] and that at 1420 cm^{-1} is stronger for the dicationic species (for which the quinoidization nearly extends over the whole molecule, due to the electrostatic repulsion between the two positive charges).^[19b] This simple Raman spectral pattern has also been found for a new class of oligothiophenes bearing a pure heteroaromatic structure in their electronic ground state.^[33, 34] The softening of the $\nu(\text{CN})$ mode is quite significant for **2b** and **5b**, what agrees with the rather low BLA value calculated in each case for the thiophene ring attached to the acceptor (i.e., -0.004 \AA for **2b** and 0.001 \AA for **5b**), indicative of a strong degree of quinoidization.

The large involvement of the nitrile groups in the ICT is clearly evidenced by the sizeable dispersion towards lower frequencies, by near $50\text{--}60\text{ cm}^{-1}$, of the IR and Raman-active $\nu(\text{CN})$ stretching vibrations of these NLO-phores, recorded at around $2210\text{--}2220\text{ cm}^{-1}$, as compared with the 2270 cm^{-1} frequency value measured for a non-conjugated dicyanomethane model system (see Figure 9 and Table 2).

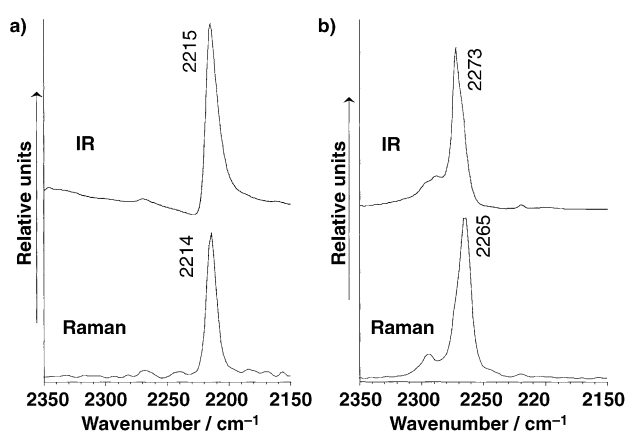


Figure 9. IR and Raman bands due to the $\nu(\text{CN})$ stretching vibrations of a) **2b** and b) $\text{CH}_2(\text{CN})_2$ as solids.

Table 2. Frequencies measured for the IR and Raman-active $\nu(\text{CN})$ stretching vibrations of **1b**, **2b**, **4b**, **5b** and $\text{CH}_2(\text{CN})_2$ as solids.

Compound	IR ^[a]	Raman ^[a]
1b	2219	2220
2b	2215	2214
4b	2216, 2205	2204
5b	2210	2208
$\text{CH}_2(\text{CN})_2$	2273	2265

[a] Frequency values in cm^{-1} .

IR and Raman Spectra of the NLO-phores as solutes in dilute solutions: Figure 10 shows the comparison of the Raman spectra of **1b**, **4b** and **5b** obtained from the pure solids and as solutes in dilute CH_2Cl_2 solutions (after properly subtracting the Raman scatterings of the pure solvent). In particular, we observed that the spectral profile of **1b** in dichloromethane

solution can be almost superposed with that recorded for the solid. In fact, only a subtle upshift of 4 cm^{-1} was observed for the characteristic \mathfrak{A} mode upon solution, when the relative intensities of the most outstanding features remain nearly unaffected. In addition, the Raman spectrum of **1b** in DMSO, although not reported here, was found to be identical to that recorded in CH_2Cl_2 . These experimental findings reveal that, in the case of **1b** and **2b**, there is not loss of π -conjugation in going from solids to solution. The two thiophene rings of **1b** are located in opposite directions with respect to the central vinylenic bridge not only in solid state but also in solution (i.e., the molecular conformation most favorable to the ICT). Nonetheless, the polar electron donor and acceptor end groups are expected to undergo some conformational distortions in the different environments due to the interaction with the solvents.

Conformational distortions in solution for **4b** and **5b** are larger than those for **1b** and **2b**. Table 3 lists the frequencies measured for the Raman bands of **4b** and **5b** in solid state and

Table 3. Comparison between the frequencies measured for the Raman bands of **4b** and **5b** in solid state and CH_2Cl_2 solution, in the $1700\text{--}1250\text{ cm}^{-1}$ spectral range.

NLO-phore	NLO-phore 4b		NLO-phore 5b	
	solid state ^[a]	CH_2Cl_2 solution ^[a]	solid state ^[a]	CH_2Cl_2 solution ^[a]
1614	1618	1615	1615	
1592	1601	1599	1600	
1564	1573	1547	1552	
1511	1534	1524	1533	
1495	1521	1493	1499	
1479	1490	1453	1471	
1428	1430	1430	1437	
1357	1367 and 1350	1358	1364	
1319	1321	1325	1329	
1291	1302	1290	1294	
1278	1278	1272	1280	
1267	1260	1265	1266	

[a] Frequency values in cm^{-1} .

CH_2Cl_2 solution. One observes that all Raman-active vibrations appearing in the $1700\text{--}1250\text{ cm}^{-1}$ spectral region, and among them those related to the π -conjugating spacer, experience a significant blueshift upon removing solid state packing forces and when intermolecular interactions between the solute and solvent enter into play (spectral differences are particularly significant for **4b**, due to the lack of the non-covalent intramolecular interactions). Following the same reasoning exposed along the Raman analysis of the NLO-phores in solid state, the upshifts of the skeletal Raman vibrations upon solution must be ascribed to a partial loss of the overall π -conjugation of the system due to sizeable conformational distortions from coplanarity, not only of the electron donating and electron withdrawing end groups (as it occurs for **1b** and **2b**) but also of the two thienyl subunits of the π -conjugated spacer. The upshift of the IR absorptions due to $\nu(\text{CN})$ stretching vibrations upon solution is also evidence for a partial gain of “triple-bond character” of the

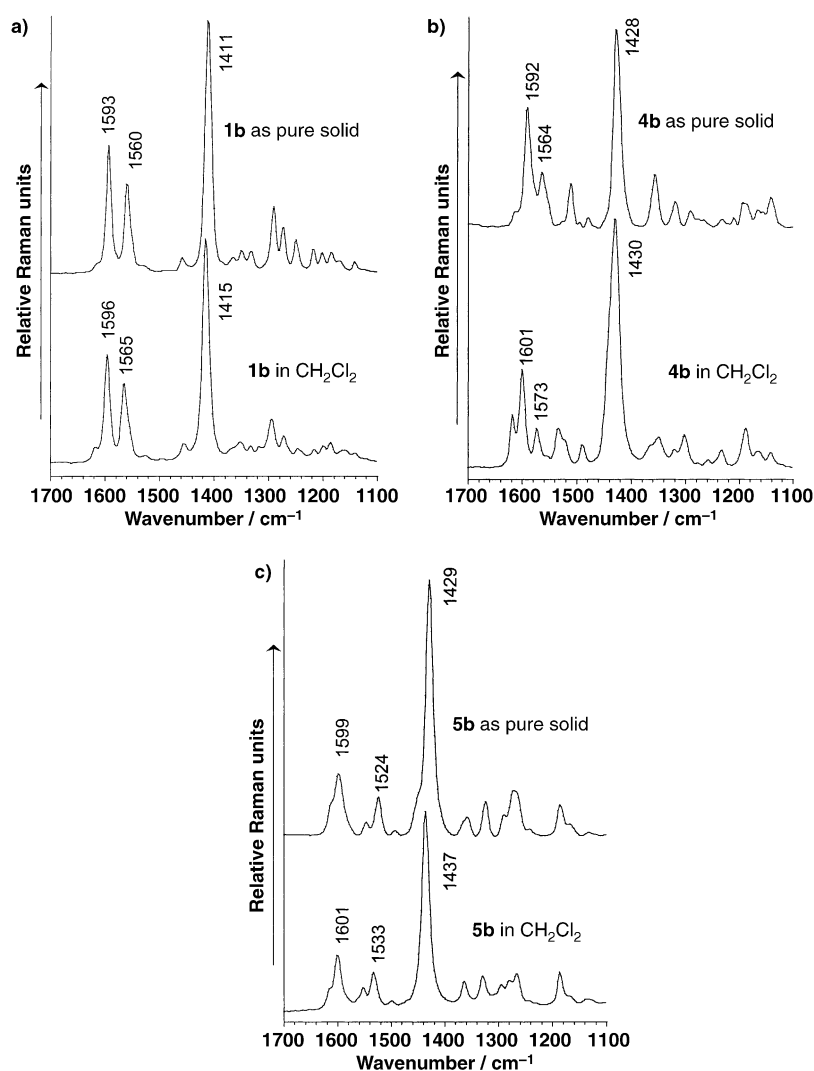


Figure 10. Comparison between Raman spectral profiles of a) **1b**, b) **4b** and c) **5b** as solids and as solutes in dilute CH_2Cl_2 solutions.

nitrile groups of the malonitrile acceptor moiety, as a consequence of the lowering of the ICT (see Figure 11). To evaluate the conformational distortion, quantum chemical calculations of the Raman spectra, at the B3LYP/3-21G* level, on a model distorted molecule of **4b** consisting on the 20° rotation around each of the single bonds that laterally connect the thiophene rings have been carried out. The wavenumbers calculated are in good agreement with the experimental observations and satisfactorily reproduce the reported dispersion toward higher energies as the chain is rotated.

The ICT of these four NLO-phores is, however, rather moderately dependent on the solvent polarity, as shown by the electronic absorption and vibrational data in various solvents. In this regard, Effenberger et al. have recently reported on the solvatochromic properties in 34 solvents of a 5-(dimethylamino)-5'-nitro-2,2'-bithiophene, for which the UV/Vis absorption maxima (λ_{max}) showed a pronounced redshift, by 130 nm, in going from *n*-pentane to a formamide/ H_2O (1:1) mixture.^[35]

Summary and Conclusion

In summary, we have described the synthesis of two novel donor–acceptor systems to complete a previously reported series of push–pull chromophores built around thiophene-based π -conjugating spacers rigidified by either covalent bonds or noncovalent intramolecular interactions. The molecular geometry optimizations performed for the four compounds reveal an interesting result which is in contrast with the classical view of a chemist for this type of push–pull molecules in terms of resonant structures: the thiophene ring attached to the electron acceptor displays a partial quinonoid-like structure while that directly connected to the electron donor still retain a partial aromatic-like structure. The B3LYP/6-31G* atomic charge distribution also indicates that the net negative charge over the malonitrile acceptor group is around three times higher than the positive charge on the *N,N*-dimethylaniline donor group, and that the π -conjugating spacer is strongly polarized since it bears nearly the 60–70% of the net positive charge of the zwitterionic form of the molecule.

The four types of D- π -A systems studied in this paper showed an intramolecular charge transfer band in their electronic absorption spectra, which is influenced by the nature of the π -conjugating spacer. The topologies and energies of the molecular orbitals were studied by means of TDDFT//B3LYP/6-31G* showing that the HOMO–LUMO energy gaps account for the observed intramolecular charge transfer from the donor subunit of the NLO-phore including the nearest thiophene unit to the acceptor subunit (i.e., mainly the electron-withdrawing malonitrile group).

The compounds have been also analysed by means of IR and Raman spectroscopies in solid state as well as in a variety of solvents. As a first result, the resemblance between the IR and Raman spectra constitutes a proof of a very effective intramolecular charge transfer. The conjugated bridge gives rise to collective normal modes (the \mathfrak{R} mode in the ECC theory) during which changes of the molecular polarizability are relevant. In the case of push–pull molecules these modes are also strongly activated in the IR spectra because the

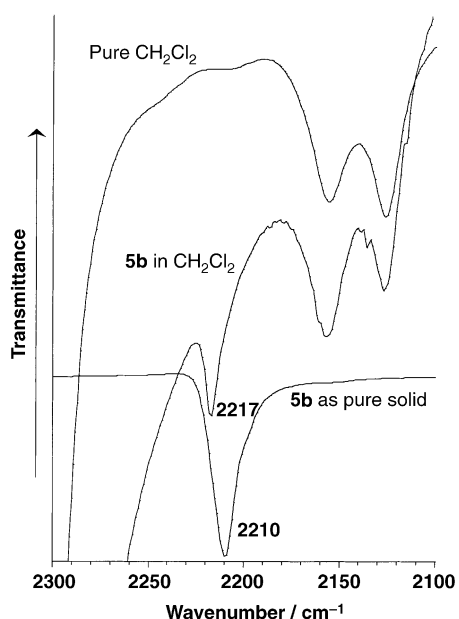


Figure 11. Comparison between the IR absorption spectra of **5b** as a pure solid and in dilute CH_2Cl_2 solution together with the background spectrum of the pure solvent in the $2300\text{--}2100\text{ cm}^{-1}$ spectral range.

polarization of the molecular backbone by the presence of polar end groups. The large intensities of these IR-active modes can be ascribed to large charge fluxes along the carbon–carbon bonds, induced by the \mathfrak{A} oscillation, which generate a very large molecular dipole moment variation directed along the chain axis. The Raman data demonstrate that the covalent rigidification of the dithienylene spacer renders a richer π -electron system (due to the strong inductive effects from the ethylene groups connecting the inner β -positions of the DTE spacer), thus improving the intramolecular charge transfer. The Raman data also suggests that the NLO-phores based on 2,2'-bi(3,4-ethylenedioxythiophene) (BEDOT) spacer display a better intramolecular charge transfer than their corresponding parent compounds based on an unsubstituted bithiophene (BT) spacer; in this case the noncovalent intramolecular interactions between sulfur and oxygen atoms appear to be responsible for the rigidification of the push–pull system.

Very subtle Raman spectral changes between solutes and solids were noticed for the NLO-phores based either on the covalently bridged or the open chain DTE spacers (i.e., for **1b** and **2b**). This experimental finding suggests that the π -conjugation is the driving force which determines that the distortions form coplanarity of the thiophene rings of DTE must be very little either in solid state or in solution. On the other hand, **4b** and **5b** NLO-phores undergo larger conformational distortions in solution with respect to the solid state (particularly in the former case). Thus, the insertion of vinylenic bridges between the thienyl subunits of the π -conjugating spacer and between the spacer and the donor and acceptor end groups seems to be a suitable strategy to reach a fairly large intramolecular charge transfer both in polar and nonpolar solvents.

Experimental and Theoretical Details

^1H and ^{13}C NMR spectra were recorded on a Bruker Avance DRX 500 spectrometer operating at 500.13 and 125.7 MHz, respectively; δ are given in ppm (relative to TMS) and coupling constants (J) in Hz. Mass spectra were recorded under positive electrospray (ESI+) on a JMS-700 JEOL mass spectrometer of reserved geometry. UV/VIS-NIR absorption spectra were recorded on a Lambda 19 Perkin–Elmer spectrometer. Melting points were obtained from a Reichert–Jung Thermovar hot-stage microscope apparatus and are uncorrected.

The FT-IR spectra were recorded on a Bruker Equinox55 spectrometer. Oligomers were ground to a powder and pressed in a KBr pellet. IR absorption measurements were also made for some NLO-phores in CH_2Cl_2 solution using a demountable liquid cell with potassium bromide windows. Spectra were collected with a spectral resolution of 2 cm^{-1} , and the mean of 50 scans was obtained. Interference from atmospheric water vapor was minimized by purging the instrument with dry argon prior to the data collection. FT-Raman spectra were collected on a Bruker FRA106/S apparatus and a Nd/YAG laser source ($\lambda_{\text{exc}} = 1064\text{ nm}$), in a back-scattering configuration. The operating power for the exciting laser radiation was kept to 100 mW in all the experiments. Samples were analyzed as pure solids in sealed capillaries as well as in dioxane, THF, CH_2Cl_2 and DMSO solutions (supplied by Aldrich with analytical grade). Typically, 1000 scans with 2 cm^{-1} spectral resolution were averaged to optimize the signal-to-noise ratio.

Density functional theory (DFT) calculations were carried out by means of the Gaussian 98 program^[36] running on SGI Origin2000 supercomputer. We used the Becke's three-parameter exchange functional combined with the LYP correlation functional (B3LYP).^[37] It has already been shown that the B3LYP functional yields similar geometries for medium-sized molecules as MP2 calculations do with the same basis sets.^[38, 39] Moreover, the DFT force fields calculated using the B3LYP functional yield IR spectra in very good agreement with experiments.^[40, 41] We also made use of the standard 3-21G* and 6-31G* basis sets.^[42, 43] Optimal geometries were determined on isolated entities. All geometrical parameters were allowed to vary independently apart from planarity of the rings. On the resulting ground-state optimized geometries, harmonic vibrational frequencies and IR and Raman intensities were calculated analytically with the B3LYP functional.

We used the frequently used adjustment of the theoretical force fields in which frequencies are uniformly scaled down by a factor of 0.98 or 0.96 for the 3-21G* and 6-31G* calculations, respectively, as recommended by Scott and Radom.^[40] This scaling procedure is often accurate enough to disentangle serious experimental misassignments. All quoted vibrational frequencies reported along the paper are thus scaled values. The theoretical spectra were obtained by convoluting the scaled frequencies with Gaussian functions (10 cm^{-1} width at the half-height). The relative heights of the Gaussians were determined from the theoretical Raman scattering activities.

Vertical electronic excitation energies were computed by using the time-dependent DFT (TDDFT) approach.^[44, 45] The twelve lowest-energy electronic excited states were at least computed for all the molecules. Numerical applications reported so far indicated that TDDFT employing current exchange–correlation functionals performs significantly better than HF-based single excitation theories for the low-lying valence excited states of both closed-shell and open-shell molecules.^[46, 47] TDDFT calculations were carried out using the B3LYP functional and the 6-31G* basis set on the previously optimized molecular geometries obtained at the same level of calculation.

(E)-1-[2-(2,2-Dicyanoethenyl)-5-thienyl]-2-[2-(E)-(4-N,N-dimethylaminobenzylidenemethyl)-5-thienyl]ethene (1b): A mixture of (E)-1-[2-(E)-(4-N,N-dimethylaminobenzylidenemethyl)-5-thienyl]-2-[2-formyl-5-thienyl]ethene (40 mg, 0.11 mmol), malonitrile (13 mg, 0.18 mmol) and one drop of Et_3N in CHCl_3 (10 mL) was heated under reflux for 18 h. The mixture was concentrated in vacuo to give a residue which was purified by chromatography on silica gel (CH_2Cl_2) to give compound **1b** as a dark blue powder (35 mg, 72%). M.p. $252\text{ }^\circ\text{C}$; ^1H NMR (CDCl_3): $\delta = 7.71$ (s, 1H), 7.56 (d, 1H, $^3J = 4.1$), 7.37 (d, 2H, $^3J = 8.8$), 7.30 (d, 1H, $^3J = 15.6$), 7.10 (d, 1H, $^3J = 4.1$), 7.06 (d, 1H, $^3J = 3.8$), 6.99 (d, 1H, $^3J = 15.9$), 6.93 (d, 1H, $^3J = 15.9$), 6.91 (d,

1H, $^3J=3.8$), 6.90 (d, 1H, $^3J=15.6$), 6.70 (d, 2H, $^3J=8.8$), 3.00 (s, 6H); ESI+ MS m/z : 413.01.

5-(2,2-Dicyanoethenyl)-5-[(E)-(4-N,N-dimethylaminobenzylidene)methyl]-2,2'-bithiophene (4b): A mixture of 5-formyl-5-[(E)-(4-N,N-dimethylaminobenzylidene)methyl]-2,2'-bithiophene (90 mg, 0.26 mmol), malononitrile (32 mg, 0.49 mmol) and one drop of Et₃N in CHCl₃ (20 mL) was heated under reflux for 18 h. The mixture was concentrated in vacuo to give a residue which was purified by chromatography on silica gel (CH₂Cl₂) to give compound **4b** as a dark blue powder (55 mg, 54%). M.p. 212 °C; ¹H NMR (CDCl₃): $\delta=7.72$ (s, 1H), 7.61 (d, 1H, $^3J=4.1$), 7.38 (d, 2H, $^3J=8.8$), 7.33 (d, 1H, $^3J=3.9$), 7.22 (d, 1H, $^3J=4.1$), 6.98 (d, 1H, $^3J=16$), 6.95 (d, 1H, $^3J=3.9$), 6.93 (d, 1H, $^3J=16$), 6.70 (d, 2H, $^3J=8.8$), 3.01 (s, 6H); ESI+ MS m/z : 387.08.

Acknowledgements

M.C.R.D., V.H., J.C. and J.T.L.N. would like to acknowledge the Dirección General de Enseñanza Superior (DGES, MEC, Spain) and the Junta de Andalucía (Spain) for financial support to the research performed at the University of Málaga through project BQU2000-1156 and grant FQM-0159. J.C. thanks to the Ministerio de Ciencia y Tecnología of Spain for a Ramón y Cajal position of chemistry at the University of Málaga. J.M.R., P.B. and J.R. would like to thank France-Telecom for financial support to the work at the University of Angers.

- [1] a) P. N. Prasad, D. J. Williams, *Introduction to Nonlinear Optical Effects in Molecules and Polymers*, Wiley, New York, **1991**; b) J. Zyss, *Molecular Nonlinear Optics: Materials, Physics and Devices*, Academic Press, Boston, **1993**; c) D. R. Kanis, M. A. Ratner, T. J. Marks, *Chem. Rev.* **1994**, *94*, 195; d) S. R. Marder, J. W. Perry, *Adv. Mater.* **1993**, *5*, 804; e) T. J. Marks, M. A. Ratner, *Angew. Chem.* **1995**, *107*, 167; *Angew. Chem. Int. Ed. Engl.* **1995**, *34*, 155; f) L. R. Dalton, A. W. Harper, R. Ghosn, W. H. Steier, M. Ziari, H. Fetterman, Y. Shi, R. V. Mustacich, A. K.-Y. Jen, K. J. Shea, *Chem. Mater.* **1995**, *7*, 1060; g) Y. Shi, C. Zhang, J. H. Bechtel, L. R. Dalton, B. H. Robinson, W. H. Steier, *Science* **2000**, *288*, 119.
- [2] a) T. Verbiest, S. Houbrechts, M. Kauranen, K. Clays, A. Persoons, *J. Mater. Chem.* **1997**, *7*, 2175; b) J. J. Wolf, R. Wortmann, *Adv. Phys. Org. Chem.*, **1999**, *32*, 121.
- [3] a) N. J. Long, *Angew. Chem.* **1995**, *107*, 37; *Angew. Chem. Int. Ed. Engl.* **1995**, *34*, 21; b) H. Le Bozec, T. Renouard, *Eur. J. Inorg. Chem.* **2000**, 229.
- [4] a) S. R. Marder, C. B. Gorman, B. G. Tiemann, L. T. Cheng, *J. Am. Chem. Soc.* **1993**, *115*, 3006; b) S. R. Marder, L. T. Cheng, B. G. Tiemann, *J. Chem. Soc. Chem. Commun.* **1992**, 672; c) L. T. Cheng, W. Tam, S. R. Marder, A. E. Steigman, G. Rikken, C. W. Spangler, *J. Phys. Chem.* **1993**, *95*, 10631 and L. T. Cheng, W. Tam, S. R. Marder, A. E. Steigman, G. Rikken, C. W. Spangler, *J. Phys. Chem.* **1993**, *95*, 10643.
- [5] a) S. R. Marder, L. T. Cheng, B. G. Tiemann, A. C. Friedli, M. Blanchard-Desce, J. W. Perry, J. Skindhoj, *Science* **1994**, *263*, 511; M. Blanchard-Desce, V. Alain, P. V. Bedworth, S. R. Marder, A. Fort, C. Runser, M. Barzoukas, M. S. Lebus, R. Wortmann, *Chem. Eur. J.* **1997**, *3*, 1091.
- [6] a) G. Mignani, F. Leising, R. Meyreux, H. Samson, *Tetrahedron Lett.* **1990**, *31*, 4743; b) A. K.-Y. Jen, V. P. Rao, K. J. Drost, K. Y. Wong, M. P. Cava, *J. Chem. Soc. Chem. Commun.* **1994**, 2057; c) V. P. Rao, Y. M. Cai, A. K.-Y. Jen, *J. Chem. Soc. Chem. Commun.* **1994**, 1689; d) A. K.-Y. Jen, Y. M. Cai, P. V. Bedworth, S. R. Marder, *Adv. Mater.* **1997**, *9*, 12.
- [7] a) V. P. Rao, A. K.-Y. Jen, K. Y. Wong, K. J. Drost, *J. Chem. Soc. Chem. Commun.* **1993**, 1118; b) S. Gilmour, R. A. Montgomery, S. R. Marder, L.-T. Cheng, A. K.-Y. Jen, Y. Cai, J. W. Perry, L. R. Dalton, *Chem. Mater.* **1994**, *6*, 1603; c) P. Boldt, G. Bourhill, C. Bräuchle, Y. Jim, R. Kammler, C. Müller, J. Rase, J. Wichern, *Chem. Commun.* **1996**, 793; d) X. Wu, J. Wu, Y. Liu, A. K.-Y. Jen, *J. Am. Chem. Soc.* **1999**, *121*, 472; e) X. Wu, J. Wu, Y. Liu, A. K.-Y. Jen, *Chem. Commun.* **1999**, 2391.
- [8] S.-S. Sun, C. Zhang, L. R. Dalton, S. M. Garner, A. Chen, W. H. Steier, *Chem. Mater.* **1996**, *8*, 2539.
- [9] A. K.-Y. Jen, Y. Liu, L. Zheng, S. Liu, K. J. Drost, Y. Zhang, L. R. Dalton, *Adv. Mater.* **1999**, *11*, 452.
- [10] a) V. P. Rao, A. K.-Y. Jen, K. Y. Wong, K. Y. Drost, *Tetrahedron Lett.* **1993**, *34*, 1747; b) V. P. Rao, K. Y. Wong, A. K.-Y. Jen, K. J. Drost, *Chem. Mater.* **1994**, *6*, 2210; c) S. Gilmour, S. R. Marder, J. W. Perry, L. T. Cheng, *Adv. Mater.* **1994**, *6*, 494; d) F. Steybe, F. Effenberger, U. Gubler, C. Bosshard, P. Günter, *Tetrahedron* **1998**, *54*, 8469; e) O.-K. Kim, A. Fort, M. Barzoukas, M. Blanchard-Desce, J.-M. Lehn, *J. Mater. Chem.* **1999**, *9*, 2227; f) C. Cai, I. Liakatas, M.-S. Wong, M. Bösch, C. Bosshard, P. Günter, S. Concilio, N. Tirelli, U. W. Suter, *Org. Lett.* **1999**, *1*, 1847; g) M. G. Hutchings, I. Ferguson, D. J. McGeein, J. O. Morley, J. Zyss, I. Ledoux, *J. Chem. Soc. Perkin Trans. 2* **1995**, 171.
- [11] a) S. R. Marder, J. W. Perry, G. Bourhill, C. B. Gorman, B. G. Tiemann, K. Mansour, *Science* **1993**, *261*, 186; S. R. Marder, C. B. Gorman, F. Meyers, J. W. Perry, G. Bourhill, J.-L. Brédas, B. M. Pierce, *Science* **1994**, *265*, 632.
- [12] a) V. P. Rao, A. K.-Y. Jen, Y. Cai, *J. Chem. Soc. Chem. Commun.* **1996**, 1237; b) K. Y. Wong, A. K.-Y. Jen, V. P. Rao, K. Drost, R. M. Minnini, *Proc. SPIE* **1992**, *74*; c) A. K.-Y. Jen, Y. Cai, P. V. Bedworth, S. R. Marder, *Adv. Mater.* **1997**, *9*, 132.
- [13] J.-M. Raimundo, P. Blanchard, I. Ledoux-Rak, R. Hierle, L. Michaux, J. Roncali, *J. Chem. Commun.* **2000**, 1597.
- [14] J.-M. Raimundo, P. Blanchard, P. Frère, N. Mercier, I. Ledoux-Rak, R. Hierle, J. Roncali, *Tetrahedron Lett.* **2001**, *42*, 1507.
- [15] J.-M. Raimundo, P. Blanchard, N. Gallego-Planas, N. Mercier, I. Ledoux-Rak, R. Hierle, J. Roncali, *J. Org. Chem.* **2002**, *67*, 205.
- [16] A. Sakamoto, Y. Furukawa, M. Tasumi, *J. Phys. Chem.* **1994**, *98*, 4635.
- [17] N. Yokonuma, Y. Furukawa, M. Tasumi, M. Kuroda, J. Nakayama, *Chem. Phys. Lett.* **1996**, *255*, 431.
- [18] a) J. Casado, V. Hernandez, S. Hotta, J. T. López Navarrete, *J. Chem. Phys.* **1998**, *109*, 10419; b) C. Moreno Castro, M. C. Ruiz Delgado, V. Hernandez, S. Hotta, J. Casado, J. T. López Navarrete, *J. Chem. Phys.* **2002**, *116*, 10419; c) C. Moreno Castro, M. C. Ruiz Delgado, V. Hernandez, Y. Shirota, J. Casado, J. T. López Navarrete, *J. Phys. Chem. B* **2002**, *106*, 7163.
- [19] a) J. Casado, T. F. Otero, S. Hotta, V. Hernandez, F. J. Ramirez, J. T. López Navarrete, *Opt. Mater.* **1998**, *9*, 82; b) J. Casado, V. Hernandez, S. Hotta, J. T. López Navarrete, *Adv. Mater.* **1998**, *10*, 1258.
- [20] V. Hernandez, J. Casado, F. Effenberger, J. T. López Navarrete, *J. Chem. Phys.* **2000**, *112*, 5105.
- [21] M. Gonzalez, J. L. Segura, C. Seoane, N. Martin, J. Garin, J. Orduna, R. Alcalá, B. Villacampa, V. Hernandez, J. T. López Navarrete, *J. Org. Chem.* **2001**, *66*, 8872.
- [22] a) G. Zerbi, C. Castiglioni, M. Del Zoppo, *Electronic Materials: The Oligomer Approach*, Wiley-VCH, Weinheim, **1998**, pp.345; C. Castiglioni, M. Gussoni, J. T. López Navarrete, G. Zerbi, *Solid State Commun.* **1988**, *65*, 625; c) J. T. López Navarrete, G. Zerbi, *J. Chem. Phys.* **1991**, *94*, 957 and J. T. López Navarrete, G. Zerbi, *J. Chem. Phys.* **1991**, *94*, 965; d) V. Hernandez, C. Castiglioni, M. Del Zoppo, G. Zerbi, *Phys. Rev. B* **1994**, *50*, 9815; e) E. Agosti, M. Rivola, V. Hernandez, M. Del Zoppo, G. Zerbi, *Synth. Met.* **1999**, *100*, 101.
- [23] a) C. Ehrendorfer, A. Karpfen, *J. Phys. Chem.* **1994**, *98*, 7492; b) C. Ehrendorfer, A. Karpfen, *J. Phys. Chem.* **1995**, *99*, 5341.
- [24] R. E. Müller, F. F. Nord, *J. Org. Chem.* **1951**, *16*, 1380.
- [25] a) J. Roncali, C. Thobie-Gautier, E. H. Elandaloussi, P. Frère, *J. Chem. Soc. Chem. Commun.* **1994**, 2249; b) P. Blanchard, H. Brisset, B. Illien, A. Riou, J. Roncali, *J. Org. Chem.* **1997**, *62*, 2401.
- [26] a) G. A. Sotzing, J. R. Reynolds, *Adv. Mater.* **1997**, *9*, 795; b) S. Akoudad, J. Roncali, *Synth. Met.* **1998**, *93*, 111.
- [27] H. Bredereck, G. Simchen, W. Griebenow, *Chem. Ber.* **1973**, *106*, 3732.
- [28] M. Turbiez, P. Frère, P. Blanchard, J. Roncali, *Tetrahedron Lett.* **2000**, *41*, 5521.
- [29] S. Hotta, K. Waragai, *J. Mater. Chem.* **1991**, *1*, 835.
- [30] F. Van Bolhuis, H. Wynberg, E. E. Havinga, E. W. Meijer, E. Staring, *Synth. Met.* **1989**, *30*, 381.
- [31] D. Fichou, *J. Mater. Chem.* **2000**, *10*, 571 and references therein.
- [32] L. L. Miller, Y. Yu, *J. Org. Chem.* **1995**, *60*, 6813.
- [33] V. Hernandez, S. Hotta, J. T. López Navarrete, *J. Chem. Phys.* **1998**, *109*, 2543.

- [34] V. Hernandez, S. Calvo Losada, J. Casado, H. Higuchi, J. T. López Navarrete, *J. Phys. Chem. A* **2000**, *104*, 661.
- [35] F. Effenberger, F. Würthner, F. Steybe, *J. Org. Chem.* **1995**, *60*, 2082.
- [36] M. J. Frisch, G. W. Trucks, H. B. Schlegel, G. E. Scuseria, M. A. Robb, J. R. Cheeseman, V. G. Zakrzewski, J. A. Montgomery, R. E. Stratman, S. Burant, J. M. Dapprich, J. M. Millam, A. D. Daniels, K. N. Kudin, M. C. Strain, O. Farkas, J. Tomasi, V. Barone, M. Cossi, R. Cammi, B. Mennucci, C. Pomelli, C. Adamo, S. Clifford, G. Ochterski, A. Petersson, P. Y. Ayala, Q. Cui, K. Morokuma, D. K. Malick, A. D. Rabuck, K. Raghavachari, J. B. Foresman, J. Cioslowski, J. V. Ortiz, B. B. Stefanov, G. Liu, A. Liashenko, I. Piskorz, I. Komaromi, R. Gomperts, R. L. Martin, D. J. Fox, T. Keith, M. A. Al-Laham, C. Y. Peng, A. Manayakkara, C. Gonzalez, M. Challacombe, P. M. W. Gill, B. G. Johnson, W. Chen, M. W. Wong, J. L. Andres, M. Head-Gordon, E. S. Replogle, J. A. Pople, *Gaussian 98, Revision A.7*, Gaussian Inc., Pittsburgh PA, **1998**.
- [37] A. D. Becke, *J. Chem. Phys.* **1993**, *98*, 1372.
- [38] P. J. Stephens, F. J. Devlin, F. C. F. Chabalowski, M. J. Frisch, *J. Phys. Chem.* **1994**, *98*, 11623.
- [39] J. J. Novoa, C. Sosa, *J. Phys. Chem.* **1995**, *99*, 15837.
- [40] A. P. Scott, L. Radom, *J. Phys. Chem.* **1996**, *100*, 16502.
- [41] G. Rauhut, P. Pulay, *J. Phys. Chem.* **1995**, *99*, 3093.
- [42] W. J. Pietro, M. M. Francl, W. J. Hehre, D. J. Defrees, J. A. Pople, J. S. Binkley, *J. Am. Chem. Soc.* **1982**, *104*, 5039.
- [43] M. M. Francl, W. J. Pietro, W. J. Hehre, J. S. Binkley, M. S. Gordon, D. J. Defrees, J. A. Pople, *J. Chem. Phys.* **1982**, *77*, 3654.
- [44] E. Runge, E. K. U. Gross, *Phys. Rev. Lett.* **1984**, *52*, 997; E. K. U. Gross, W. Kohn, *Adv. Quantum Chem.* **1990**, *21*, 255; Density Functional Theory: Proceedings of the NATO Advanced Study Institute (Eds.: E. K. U. Gross, R. M. Dreizler), Plenum Press, New York, **1995**, pp. 149.
- [45] M. E. Casida in *Recent Advances in Density Functional Methods, Part I* (Ed.: D. P. Chong), World Scientific, Singapore, **1995**, pp. 115.
- [46] W. Koch, M. C. Holthausen, *A Chemist's Guide to Density Functional Theory*, Wiley-VCH, Weinheim, **2000**.
- [47] J. Casado, L. L. Miller, K. R. Mann, T. M. Pappenfus, Y. Kanemitsu, E. Ortí, P. M. Viruela, R. Pou-Américo, V. Hernandez, J. T. López Navarrete, *J. Phys. Chem. B* **2002**, *106*, 3872.

Received: October 30, 2002
Revised: February 17, 2003 [F4542]